

# 1 Estimating the genetic parameters of yield-related 2 traits under different nitrogen conditions in maize

3 Semra Palali Delen<sup>1,2,†</sup>, Gen Xu<sup>1,2,†</sup>, Jenifer Velazquez-Perfecto<sup>3</sup>, and Jinliang Yang<sup>1,2,\*</sup>

4 <sup>1</sup>Department of Agronomy and Horticulture, University of Nebraska-Lincoln, Lincoln, NE 68583, USA

5 <sup>2</sup>Center for Plant Science Innovation, University of Nebraska-Lincoln, Lincoln, NE 68583, USA

6 <sup>3</sup>Department of Agricultural Leadership, Education and Communication, University of Nebraska-Lincoln, Lincoln,  
7 NE 68583, USA

8 <sup>†</sup>These authors contributed equally to this work.

9 <sup>\*</sup>Corresponding author: [jinliang.yang@unl.edu](mailto:jinliang.yang@unl.edu)

## 10 ABSTRACT

Understanding the genetic basis responding to nitrogen (N) fertilization in crop production is a long-standing research topic in plant breeding and genetics. Albeit years of continuous efforts, the genetic architecture parameters, such as heritability, polygenicity, and mode of selection, underlying the N responses in maize remain largely unclear. In this study, about  $n = 230$  maize inbred lines were phenotyped under high N (HN) and low N (LN) conditions for two consecutive years to obtain six yield-related traits. Heritability analyses suggested that traits highly responsive to N treatments were less heritable. Using publicly available SNP genotypes, the genome-wide association study (GWAS) was conducted to identify  $n = 231$  and  $n = 139$  trait-associated loci (TALs) under HN and LN conditions, respectively, and  $n = 162$  TALs for N-responsive (NR) traits. Furthermore, genome-wide complex trait Bayesian (GCTB) analysis, a method complementary to GWAS, was performed to estimate genetic parameters, including genetic polygenicity and the mode of selection ( $S$ ). GCTB results suggested that the NR value of a yield component trait was highly polygenic and that four NR traits exhibited negative correlations between SNP effects and their minor allele frequencies (or the  $S$  value  $< 0$ ) — a pattern consistent with negative selection to purge deleterious alleles. This study reveals the complex genetic architecture underlying N responses for yield-related traits and provides insights into the future direction for N resilient maize development.

## 12 Introduction

13 Nitrogen (N), as a fundamental macronutrient, is a major constituent of proteins, nucleic acid, and metabolites and is critical for  
14 the high yielding of crops (1). Since the 1960s, subsequent to the Green Revolution, due to the Haber-Bosch process, inorganic  
15 N fertilizers became increasingly available for crop production, especially in maize, where about 20% of the N fertilizers was  
16 applied for maize production (2; 3). However, inefficient N usage causes ammonia emission to the environment, accounting  
17 for a considerable proportion of fine particulate matter pollution (i.e., PM2.5) and reducing human population life span (4).  
18 Meanwhile, N runoff imposes substantial adverse effects on natural ecosystems, such as reduced water quality and impaired  
19 soil health. Therefore, understanding the plant response to N in crop production is crucial for human health, food security, and  
20 environmental sustainability and is a long-standing research topic in plant breeding and genetics.

21 To identify N-responsive genetic loci, many QTL studies were performed, resulting in a number of trait-associated QTLs  
22 under different N conditions (5; 6) or QTLs for different N-related traits, i.e., grain N yield, N remobilization, and post-silking  
23 N uptake (7; 8). Recently, as the technical advances, genetic studies for N-related traits shifted from QTL mapping to GWAS  
24 (9; 10), leading to high-resolution mapping results. For example, a recent GWAS using 411 maize inbred lines under optimum  
25 and low N conditions detected about 80 significant SNPs and 136 putative candidate genes (11). These N-related QTLs and  
26 trait-associated SNPs provide opportunities to investigate the fate of the deleterious alleles — the alleles can potentially affect  
27 fitness under different N conditions. During the recent maize improvement process, an excess of the mutational load was  
28 enriched in even elite maize inbred lines (12). However, it is largely unclear how many alleles contribute to NR traits and what  
29 is the mode of selection on these alleles, including potentially deleterious alleles, in affecting N responses.

30 In the current study, by employing two complementary approaches — GWAS and GCTB (Genome-wide Complex Trait  
31 Bayesian analysis), we analyzed yield-related traits collected under low N (LN) and high N (HN) conditions (i.e., trait *per se*)  
32 as well as the transformed N-responsive (NR) traits. We found higher heritability for most traits *per se* under HN than LN and  
33 identified 1,292 trait-associated SNPs in total that locate in 481 genomic regions. Inferring from genome-wide non-zero effects  
34 SNPs, including not only significant GWAS SNPs but also SNPs with minor effects, GCTB results suggested the yield-related  
35 NR traits were highly polygenic and that NR traits were more likely under negative selection (13). The complex genetic

36 architecture revealed from this study, especially for the NR traits, provides guidelines for further genome-enabled selection  
37 modeling and N resilient maize development.

## 38 Materials and Methods

### 39 Plant materials and field experimental design

40 In this experiment, a subset ( $n = 226$  genotypes) of the maize diversity panel (14) was planted in a rain-fed experimental field  
41 followed commercial maize. For the N treated plots, urea (dry fertilizer) as a source of N was applied at the rate of 120 lbs/acre  
42 before planting. The field experiment was conducted using an incompletely randomized block design in two consecutive field  
43 seasons (2018-2019). For each replication of a treatment, the field was split into four blocks by plant height and maturity (i.e.,  
44 tall/early, tall/late, short/early, short/late). Each block was further subdivided into three sub-blocks. Within each sub-blocks,  
45 two hybrid varieties B73×Mo17 and B37×Mo17 were planted randomly as check plants (see also (15; 16)).

### 46 Phenotypic data collection

47 From each two-row plot, three mature ears were harvested from the representative plants. These harvested ears were dried  
48 in the oven at 37°C for three days to decrease the moisture content. Harvested ears were hand-shelled to prevent kernel loss.  
49 After shelling, the kernels and cobs were kept separately with proper barcoded labels. From the cobs, cob diameter (CD), cob  
50 length (CL), and cob weight (CW) were manually measured. The total kernel weight (TKW) of each ear was measured from  
51 the collected kernels. And then, 20 representative kernels were selected to measure 20 kernel weight (20KW). Finally, the  
52 kernel count (KC) was computed using TKW divided by average kernel weight.

### 53 Best linear unbiased prediction (BLUP) and N-responsive trait calculation

54 To obtain the best linear unbiased prediction (BLUP) values of each genotype, we fitted a linear mixed model by treating the  
55 genotype, year, replication, block, sub-block, and genotype by year interaction as random effects. For each N treatment, the  
56 BLUP values were calculated separately using an R package “lme4” (17).

57 In the model,

$$y_{ijkrl} = \mu + g_i + t_l + g_i * t_l + b_{jrl} + s_{jkrl} + q_{rl} + \epsilon$$

58 where  $y_{ijkrl}$  is the phenotypic value of the  $i^{th}$  genotype evaluated in the  $k^{th}$  sub-block of the  $j^{th}$  block of the  $r^{th}$  replicate nested  
59 within the  $l^{th}$  year;  $\mu$  is the overall mean;  $g_i$  is the random effect of the  $i^{th}$  genotype;  $t_l$  is the random effect of the  $l^{th}$  year;  $g_i * t_l$   
60 is the random effect of the  $i^{th}$  genotype with the  $l^{th}$  year interaction;  $b_{jrl}$  is the random effect of the  $j^{th}$  block of the  $r^{th}$  replicate  
61 within the  $l^{th}$  year;  $s_{jkrl}$  is the random effect of the  $k^{th}$  sub-block of the  $j^{th}$  block of the  $r^{th}$  replicate within the  $l^{th}$  year;  $q_{rl}$  is  
62 the random effect of the  $r^{th}$  replicate nested within the  $l^{th}$  year;  $\epsilon$  is the random residual error.

63 The N-responsive (NR) traits were calculated from the BLUP values using the equation (18):

$$NR = \frac{T_{HN} - T_{LN}}{T_{LN}}$$

64 where  $T_{HN}$  and  $T_{LN}$  are the BLUP values for a given trait measured from HN and LN field conditions.

### 65 Broad sense heritability calculation

66 The broad-sense heritability ( $H^2$ ) of yield-related traits was calculated using the equation as:

$$H^2 = \frac{V_G}{V_G + \frac{V_{G \times E}}{i} + \frac{V_E}{i \times j}}$$

67 where  $V_G$  is the genotypic variance;  $V_E$  is the environmental variance of different years; and  $V_{G \times E}$  is the variance of genotype  
68 by year interaction;  $i = 2$  is the number of years and  $j = 2$  is the number of replications per year.

### 69 Genome-wide Association Study (GWAS)

70 The SNP genotype of the maize diversity panel was downloaded from maize HapMap3 (19) with AGPv4 coordinates. After  
71 filtering out SNPs with minor allele frequency (MAF)  $< 0.05$  and missing rate  $< 0.3$  among the 226 lines phenotyped in this  
72 study, approximately 21 million SNPs were retained.

73 In GWAS, we employed the QK model that considers both population structure (Q) and kinship relatedness (K) to control  
74 for multiple levels of confounding effects (20; 21). In the model,

$$\mathbf{y} = \mathbf{Qv} + \mathbf{w}_i m_i + \mathbf{Zu} + \mathbf{e}$$

74 where  $\mathbf{y}$  is a vector of BLUP value for a given trait (or the NR trait);  $\mathbf{Q}$  is the design matrix of the population structure (i.e., the  
75 principle components);  $\mathbf{v}$  is the vector of the fixed subpopulation effect;  $\mathbf{w}_i$  is a vector of the  $i^{th}$  SNP genotype;  $m_i$  is the fixed  
76 SNP effect to be estimated by an iterative procedure;  $\mathbf{Z}$  is the covariance matrix or the kinship matrix of inbred lines;  $\mathbf{u}$  is the  
77 vector of breeding values to be predicted (random effect);  $\mathbf{e}$  is the vector of the random residual error.

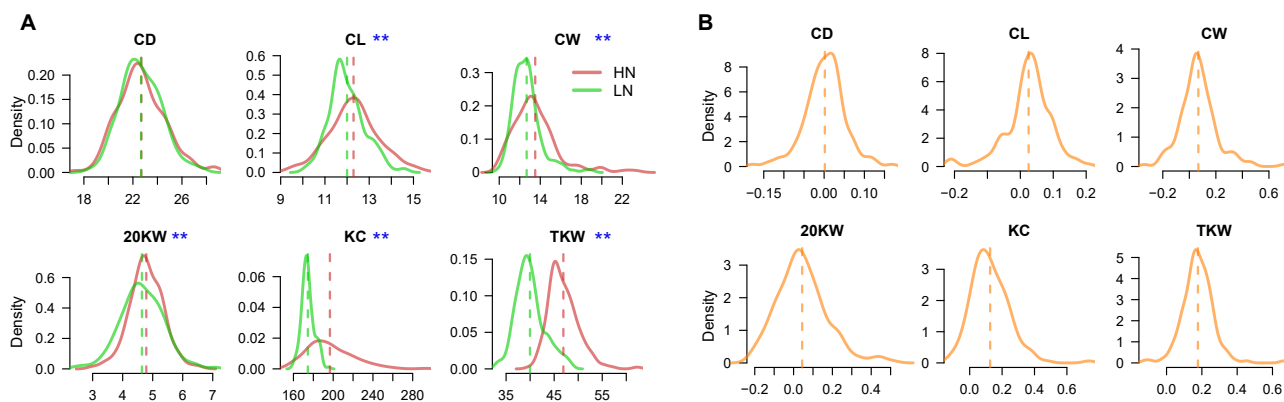
78 In the analysis, the  $\mathbf{Q}$  matrix was the first three principal components calculated from genome-wide SNPs using PLINK 1.9  
79 software (22). And the  $\mathbf{Z}$  matrix was computed using GEMMA (v 0.98.3) software with option "4" (23). The above model  
80 was then implemented to estimate significant SNP effects for each trait using GEMMA (23). The threshold for the significant  
81 association SNPs was set to  $1.2 \times 10^{-6}$  ( $1/n, n = 769,690$  is the number of independent SNPs with MAF  $\geq 5\%$ ) according to  
82 the method developed previously (15). From the GWAS results, significant genomic loci were determined by considering a  
83 100 kb window upstream and downstream of the significant SNPs. Overlapping regions were merged, and these regions were  
84 defined as trait-associated loci (TAL).

## 85 Genome-wide Complex Trait Bayesian (GCTB) analysis

86 Genome-wide Complex Trait Bayesian (GCTB-BayesS) approach, which is based on Bayesian multiple regression mixed  
87 linear models (24), was performed to estimate genetic architecture parameters of yield-related traits, including polygenicity  
88 (number of non-zero SNPs) and selection coefficient (the joint distribution between the variance of SNP effects and minor  
89 allele frequencies). Default options were selected with the following MCMC settings: "-chain-length = 1,010,000, -burn-in =  
90 10,000". In the analysis,  $n = 834,975$  independent SNPs (MAF  $\geq 1\%$ ) were used (25), which was determined by using PLINK  
91 1.9 (22) with the "indep-pairwise" option (window size 100 kb, step size 100,  $r^2 \geq 0.1$ ).

## 92 Results

### 93 Phenotypic evaluation of diverse maize lines under different N conditions



94 **Figure 1. Cob- and kernel-related traits under different N conditions.** (A) Density plots of the phenotypic traits in low N  
95 (LN) and high N (HN) fields. The red and green vertical dashed lines indicate the mean values of each trait. The blue asterisks  
96 indicate the traits show significant differences between HN and LN conditions (Paired t-test,  $P$ -value  $< 0.01$ ). (B) The  
97 distributions of N-responsive (NR) traits. Orange dashed lines denote the mean values.

98 A subset of the maize diversity panel ( $n = 226$  lines) was planted in a replicated field trial under high N (HN) and low N  
99 (LN) conditions according to an incomplete block design in 2018 and 2019 (see **Materials and Methods**). From the harvested  
100 mature ears, six yield-related traits were manually measured, including three cob-related traits (cob diameter, CD; cob length,  
101 CL; and cob weight, CW) and three kernel-related traits (20 kernel weight, 20KW; kernel count, KC; and total kernel weight,  
102 TKW). For these traits, the best linear unbiased prediction (BLUP) values were calculated separately for each N condition.  
103 Besides traits *per se*, we also calculated N-responsive (NR) traits from the BLUP values following a previous method (26) (see  
104 **Materials and Methods** and **Table S1**).

105 As expected, most of these yield-related traits exhibited significantly larger BLUP values in HN than LN conditions, except  
106 for CD (**Figure 1A**). TKW, a trait most closely related to yield (12), showed the most striking differences from 39.9 g in LN to  
107 46.9 in HN (Paired t-test,  $P$ -value =  $1.9 \times 10^{-69}$ ) and 97.8% of the lines exhibited positive N responses (**Figure 1B**). Similarly,  
108 the BLUP values for the other two kernel-related traits were also significantly improved from LN to HN, i.e., from 4.6 g to 4.8  
109 g for 20KW (Paired t-test,  $P$ -value =  $4 \times 10^{-4}$ ) and from 174 to 196 for KC (Paired t-test,  $P$ -value =  $3.9 \times 10^{-32}$ ). And 63.3%  
110 and 88.6% of the inbred lines positively responded to the elevated N levels for 20KW and KC, respectively (**Figure 1B**). For

107 cob-related traits, the phenotypic differences between HN and LN were relatively minor; for example, there were no significant  
 108 differences for CD between LN and HN (Paired t-test,  $P$ -value = 0.75).

109 **Strong N-responsive traits are less heritable**

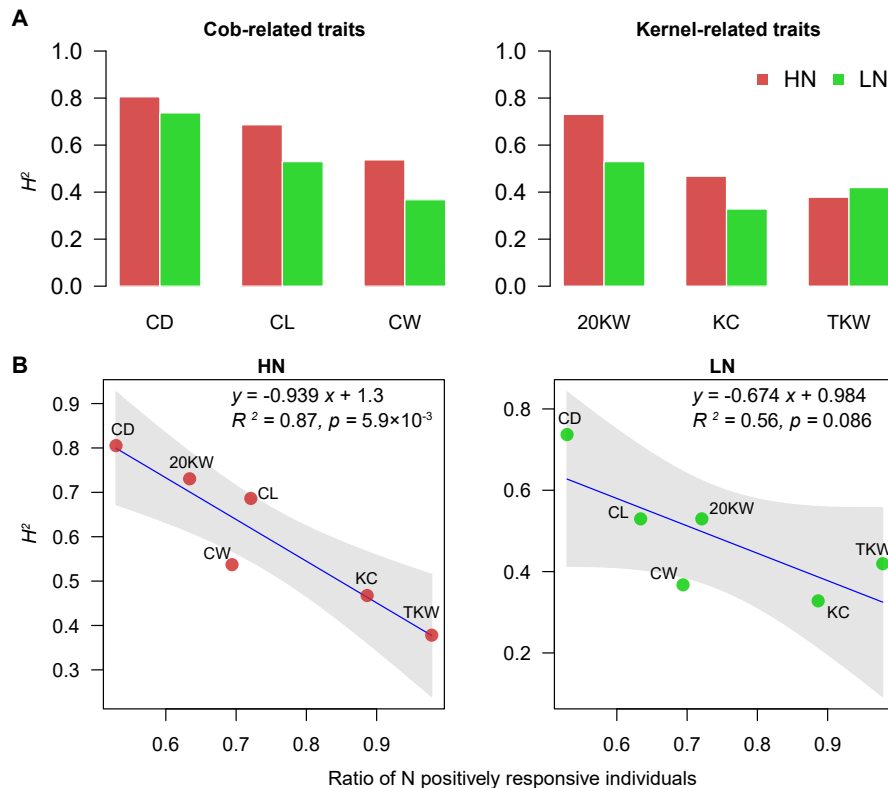


**Figure 2. Heritability estimation and correlation analysis with N-response.** (A) Heritabilities of yield-related traits under different N conditions. (B) Correlation analysis between heritability and N-responsive value. Solid blue line indicates the linear regression and the grey shaded area denotes the 95% confidence interval.

110 The broad-sense heritability ( $H^2$ ) of these yield-related traits was estimated separately for each N condition (see **Materials**  
 111 and **Methods**). Generally, we found these traits showed higher levels of heritability in HN than LN fields (**Figure 2A**), except  
 112 for TKW ( $H^2 = 0.38$  in HN and  $H^2 = 0.42$  in LN), suggesting the environmental effects were less dominant or the data were  
 113 more repeatable under HN conditions. For cob-related traits, CD ( $H^2 = 0.81$  in HN and  $H^2 = 0.74$  in LN) was more heritable  
 114 than CL ( $H^2 = 0.69$  in HN and  $H^2 = 0.53$  in LN) and CW ( $H^2 = 0.54$  in HN and  $H^2 = 0.37$  in LN); while for kernel-related  
 115 traits, 20KW ( $H^2 = 0.73$  in HN and  $H^2 = 0.53$  in LN) exhibited the highest heritability compared to KC ( $H^2 = 0.47$  in HN and  
 116  $H^2 = 0.33$  in LN) and TKW. Additionally, we found the cob-related traits, on average, were more heritable than kernel-related  
 117 traits, regardless of the N conditions (**Figure 2A**). Interestingly, the levels of heritability negatively correlated with proportions  
 118 of inbreds with NR values  $> 0$  (**Figure 1B**), or ratios of inbreds positively responding to N treatments, under both N conditions  
 119 (**Figure 2B**). These results are consistent with the view that more fitness-related traits, i.e., traits strongly responsive to N  
 120 treatments, are less heritable (27).

121 **Comparing GWAS signals under different N conditions**

122 We then conducted GWAS for the six yield-related traits *per se* as well as the transformed NR traits by fitting a linear mixed  
 123 model using 21 million SNPs (see **Materials and Methods**). In the GWAS model, the first three principal components were  
 124 fitted as the fixed effects and the genetic relatedness computed from genome-wide SNPs as the random effects. To control for  
 125 the false discovery rate (FDR), the modified Bonferroni-adjusted threshold was determined as  $1.2 \times 10^{-6}$  based on  $n = 769,690$   
 126 independent SNPs (28; 29). As a result (see **Figure S1, S2** for the quantile-quantile (Q-Q) plots), a total of 1,292 SNPs hitting  
 127 481 unique genomic regions were identified as the trait-associated loci (TALs, see **Table S2 - S3** for GWAS results).

128 We compared the shared TALs by different traits and treatments. For HN traits, in total, we identified 231 TALs (**Figure 3A**),  
 129  $n = 25$  of which were detected for at least two yield-related traits (**Figure 3B**) — more than expected by chance (permutation

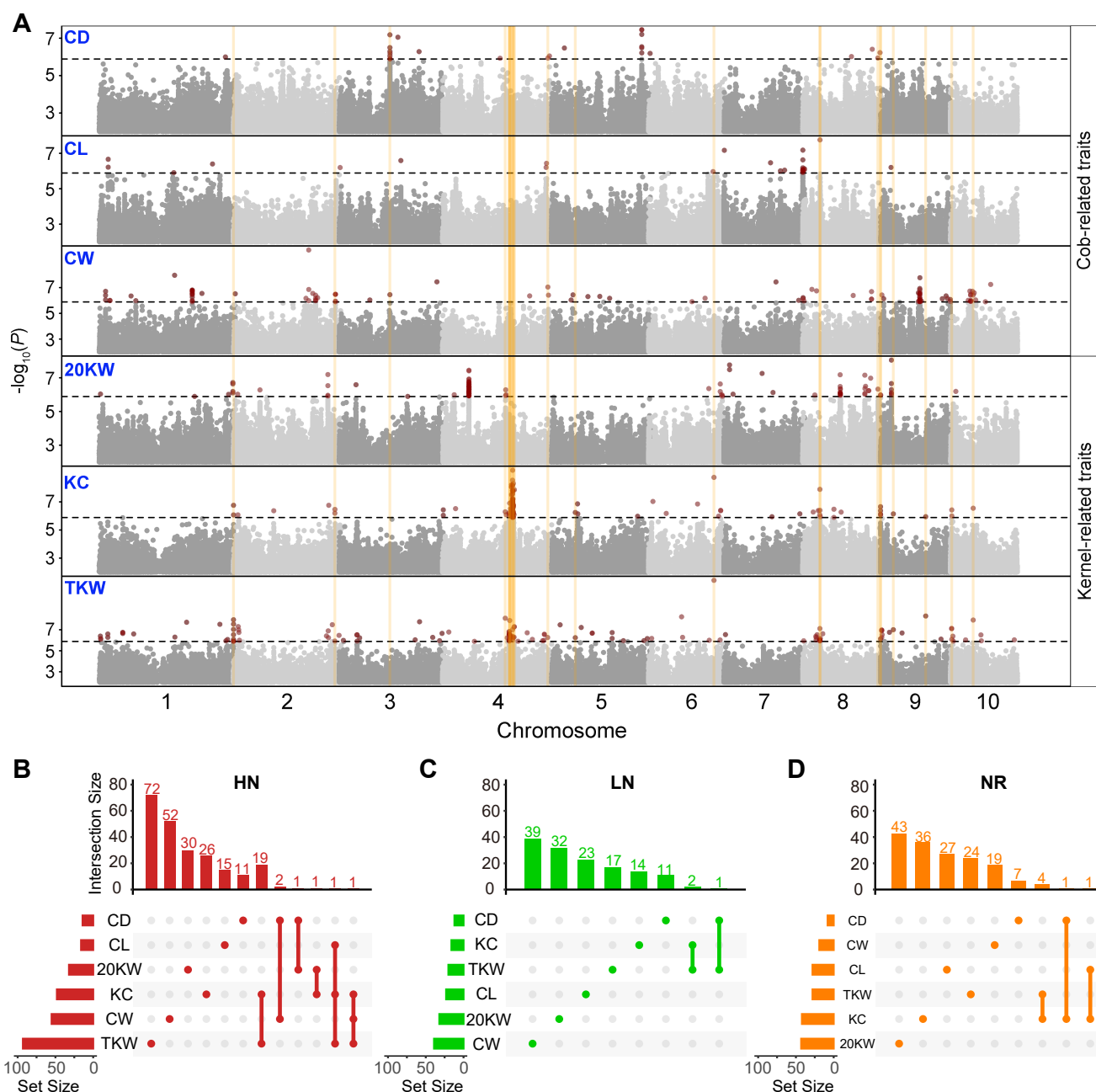


**Figure 3. GWAS results for cob- and kernel-related traits under different nitrogen conditions.** (A) Stacking Manhattan plot of cob- and kernel-related traits under HN conditions. The black horizontal dashed line indicates the GWAS threshold. Each red dot above the threshold represents the SNP significantly associated with a trait. The vertical orange lines indicate the overlapped trait-associated loci (TALs). (B-D) Overlapping results of TALs for HN (B), LN (C), and NR traits (D). Numbers on top of the barplots indicate the number of unique (only dots) and shared (dots and lines) TALs.

130 test,  $P$ -value = 0.001). Such a large number of overlapping signals were not found for LN ( $n = 3$  shared TALs, **Figure S4**) and  
 131 NR ( $n = 6$  shared TALs, **Figure S5**) traits (**Figure 3C-D**). Note that many shared TALs were between KC and TKW, likely  
 132 because KC was not a directly measured trait but calculated from TKW and 20KW. Comparatively, very few overlapped TALs  
 133 were identified for the same trait under different N conditions (**Figure S3**).

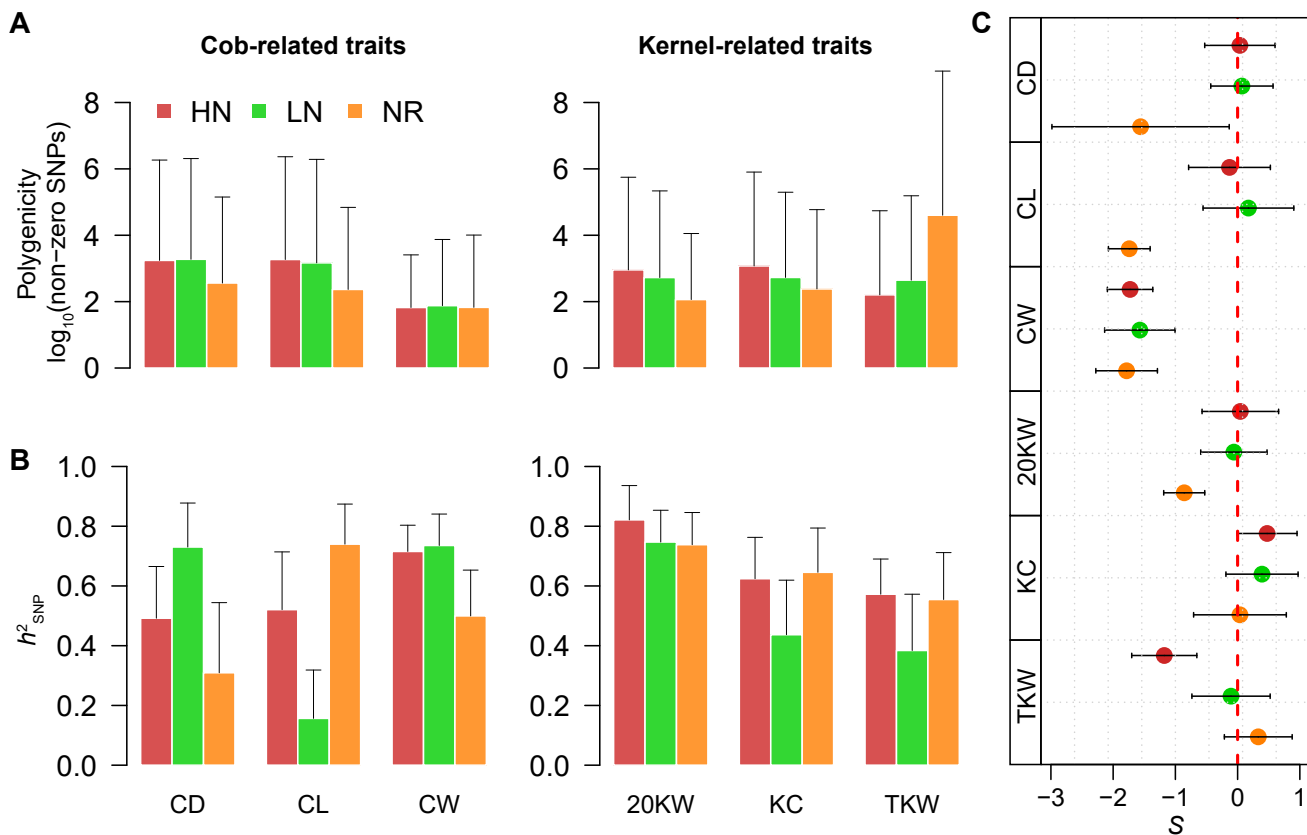


**Figure 4. Genetic architecture parameters estimated for HN, LN and NR traits.** (A) Genetic polygenicity measured by number of non-zero effect SNPs. (B) Phenotypic variance explained by SNPs under a additive model. (C) The relationships between SNP effects and MAFs of the non-zero effect SNPs.

134 **Estimating genetic architecture parameters for traits *per se* and N-responsive traits**

135 In addition to GWAS, we fitted the *per se* and NR traits to a Bayesian-based model implemented in GCTB (24). This method  
 136 allows the simultaneous estimation of the genetic architecture parameters, such as polygenicity ( $\pi$ , the percentage of non-zero  
 137 effect SNPs), variance of BLUP values due to SNPs ( $h_{SNP}^2$ , SNP-based heritability), and the mode of selection ( $S$ , a proxy using  
 138 the relationship between variance of SNP effect and MAF). Using relatively independent SNPs with MAF > 1%, we estimated  
 139 genetic parameters to compare the genetic architecture for the cob and kernel-related traits as well as for *per se* and NR traits  
 140 (see **Materials and Methods**).

141 For trait *per se* under HN and LN conditions, we observed no significant differences in the polygenicity (Figure 4A),  
 142 with an average of  $n = 906$  SNPs (or  $\pi = 0.1\%$ ) exhibiting non-zero effects; but the polygenicity among traits showed a large  
 143 variation, ranging from  $n = 66$  SNPs for CW in HN to  $n = 1,885$  SNPs for CD in LN. In particular, for the NR trait of TKW,  
 144 the number of non-zero effect SNPs elevated to  $n = 40,145$  (or  $\pi = 4.8\%$ ), suggesting TKW — a key yield component trait  
 145 — was under complex genetic control in responding to changed N conditions. The  $h_{SNP}^2$  values for HN and LN traits were  
 146 largely in line with the broad sense heritabilities estimated previously with the field data (Figure 4B). However, some abnormal  
 147 values were detected, such as a small  $h_{SNP}^2$  value for CL trait in LN, which was likely due to dominance or epistasis mode of  
 148 inheritance playing an important role as our model considered only additive effect. Or simply because of imperfect model  
 149 convergence. We also estimated the  $h_{SNP}^2$  for NR traits and found, in general, kernel-related NR traits ( $h_{SNP}^2$  ranging from  
 150  $0.55 \pm 0.15$  to  $0.73 \pm 0.1$ ) were more heritable than cob-related NR traits ( $h_{SNP}^2$  ranging from  $0.3 \pm 0.23$  to  $0.73 \pm 0.13$ ). Finally,  
 151 these estimated SNP effects and their allele frequencies in the population allowed us to infer the mode of selection. As pointed  
 152 out by Zeng et. al. (24),  $S = 0$  indicates selective neutral, while  $S > 0$  and  $S < 0$  suggest the positive and negative selection.  
 153 Our results revealed that  $S$  values of four NR traits (CD, CL, CW, and 20KW), two HN traits (CW and TKW), and one LN trait  
 154 (CW) were significantly smaller than zero (Figure 4C), indicating negative selection may be taken into effect to maintain the  
 155 large effect deleterious SNPs in low frequencies, especially in responding to changed N conditions.

## 156 Discussion

157 In this study, we characterized six yield-related traits under high and low N conditions for two consecutive years and analyzed  
158 the data with two complementary approaches — GWAS (to estimate significant effect SNPs) and GCTB (to detect non-zero  
159 effect SNPs and infer other genetic parameters). We identified 1,292 GWAS signals located within  $n = 481$  genomic regions  
160 or TALs. Many of these TALs were repeatedly detected for different traits under the same N conditions, but very few TALs  
161 were shared for the same trait under different N conditions, likely because genotype by N interaction plays an important role in  
162 controlling phenotypic variation. In addition to the GWAS SNPs, non-zero effect SNPs estimated from GCTB provided a proxy  
163 for evaluating genetic polygenicity. Results suggested that most of these yield-related traits are highly polygenic. In particular,  
164 we found the N-responsive trait of TKW was controlled by the highest number of non-zero SNPs (i.e., more than  $n = 4 \times 10^4$   
165 SNPs across the genome), consistent with the view that genetic basis for N responses in crop yield is highly complex (30).  
166 Heritability estimation from the field data suggested that traits highly responsive to N treatment tend to be less heritable, further  
167 confirming the genetic complexity of N responses for yield-related traits.

168 In the GCTB result, we detected most of the NR traits exhibiting negative S values, suggesting large effect SNPs for NR  
169 traits tend to be rare in the population. It is likely because these rare SNPs were deleterious and, therefore, were maintained in  
170 low frequencies to increase the plant fitness in responding to changed N conditions. N, as one of the significant macronutrients  
171 for crop development, its composition in the soil varies spatially and temporally (31; 32). Therefore, it is not surprising to  
172 expect plant breeding over the past 60 years since the Green Revolution or natural selection on a longer time scale has affected  
173 the patterns of deleterious alleles in responding to the N availability. However, the limitations of the current statistical methods  
174 (i.e., high false discovery rates and imperfect model convergence) prevent us from pinning down the individual deleterious  
175 locus accurately. Note that these genetic parameters were rough estimations derived from the posterior distributions. The point  
176 estimations were associated with large standard errors. To get more accurate results, a larger population or more sophisticated  
177 statistical approaches are warranted.

## 178 Data and code availability

179 The code used for the analyses can be accessed through the GitHub repository  
180 (<https://github.com/jyanglab/Genetics-parameters-for-N-related-traits>).

## 181 Acknowledgements

182 This work is supported by the Agriculture and Food Research Initiative Grant number 2019-67013-29167 from the USDA  
183 National Institute of Food, the National Science Foundation under award number OIA-1557417 for Center for Root and  
184 Rhizobiome Innovation (CRRI), and Agriculture and the University of Nebraska-Lincoln Start-up fund. This work was  
185 conducted using the Holland Computing Center of the University of Nebraska-Lincoln, which receives supports from the  
186 Nebraska Research Initiative.

## 187 Author contributions

188 J.Y. designed this work. S.P.D. and J.V.-P. generated the data. S.P.D., G.X., and J.Y. analyzed the data. S.P.D., G.X., and J.Y.  
189 wrote the manuscript.

## 190 Competing interests

191 The authors declare no competing interest.

## 192 References

- 193 1. Pilbeam, D. J. The utilization of nitrogen by plants: a whole plant perspective. *Ann. Plant Rev. Online* 305–351, DOI: 10.1002/9781444328608.ch13 (2018).
- 194 2. Heffer, P. Assessment of fertilizer use by crop at the global level 2010-2010/11 international fertilizer industry association (ifa), paris, france (2013).
- 195 3. Ludemann, C., Gruere, A., Heffer, P. & Dobermann, A. Global data on fertilizer use by crop and by country, DOI: 10.5061/dryad.2rbnzs7qh (2022).
- 196 4. Gu, B. *et al.* Abating ammonia is more cost-effective than nitrogen oxides for mitigating pm2. 5 air pollution. *Science* **374**, 758–762 (2021).
- 197 5. Agrama, H., Zakaria, A., Said, F. & Tuinstra, M. Identification of quantitative trait loci for nitrogen use efficiency in maize. *Mol. Breed.* **5**, 187–195 (1999).
- 198 6. Liu, R. *et al.* Mining of candidate maize genes for nitrogen use efficiency by integrating gene expression and qtl data. *Plant Mol. Biol. Report.* **30**, 297–308 (2012).
- 199 7. Coque, M., Martin, A., Veyrieras, J., Hirel, B. & Gallais, A. Genetic variation for n-remobilization and postsilking n-uptake in a set of maize recombinant inbred lines. 3. qtl detection and coincidences. *Theor. Appl. Genet.* **117**, 729–747, DOI: 10.1007/s00122-008-0815-2 (2008).
- 200 8. Li, P. *et al.* A genetic relationship between nitrogen use efficiency and seedling root traits in maize as revealed by QTL analysis. *J. Exp. Bot.* **66**, 3175–3188, DOI: 10.1093/jxb/erv127 (2015). <https://academic.oup.com/jxb/article-pdf/66/11/3175/17136978/erv127.pdf>.
- 201 9. Morosini, J. S. *et al.* Association mapping for traits related to nitrogen use efficiency in tropical maize lines under field conditions. *Plant Soil* **421**, 453–463 (2017).
- 202 10. He, K. *et al.* Mining of candidate genes for nitrogen use efficiency in maize based on genome-wide association study. *Mol. Breed.* **40**, 1–17, DOI: 10.1007/s11032-020-01163-3 (2020).
- 203 11. Ertiro, B. T. *et al.* Genetic dissection of nitrogen use efficiency in tropical maize through genome-wide association and genomic prediction. *Front. Plant Sci.* **11**, DOI: 10.3389/fpls.2020.00474 (2020).
- 204 12. Yang, J. *et al.* Incomplete dominance of deleterious alleles contributes substantially to trait variation and heterosis in maize. *PLoS genetics* **13**, e1007019 (2017).
- 205 13. Charlesworth, D., Charlesworth, B. & Morgan, M. The pattern of neutral molecular variation under the background selection model. *Genetics* **141**, 1619–1632 (1995).
- 206 14. Flint-Garcia, S. A. *et al.* Maize association population: a high-resolution platform for quantitative trait locus dissection. *The Plant J.* **44**, 1054–1064, DOI: <https://doi.org/10.1111/j.1365-313X.2005.02591.x> (2005). <https://onlinelibrary.wiley.com/doi/pdf/10.1111/j.1365-313X.2005.02591.x>.
- 207 15. Rodene, E. *et al.* A uav-based high-throughput phenotyping approach to assess time-series nitrogen responses and identify trait-associated genetic components in maize. *The Plant Phenome J.* **5**, e20030, DOI: <https://doi.org/10.1002/ppj2.20030> (2022). <https://acsess.onlinelibrary.wiley.com/doi/pdf/10.1002/ppj2.20030>.
- 208 16. Meier, M. A. *et al.* Association analyses of host genetics, root-colonizing microbes, and plant phenotypes under different nitrogen conditions in maize. *eLife* **11**, e75790, DOI: 10.7554/eLife.75790 (2022).
- 209 17. Bates, D., Maechler, M., Bolker, B. & Walker, S. Mixed-effects models using lme4. *J Stat Softw* **67**, 1–48 (2015).
- 210 18. Xu, G., Fan, X. & Miller, A. J. Plant nitrogen assimilation and use efficiency. *Annu. review plant biology* **63**, 153–182 (2012).
- 211 19. Bukowski, R. *et al.* Construction of the third-generation Zea mays haplotype map. *GigaScience* **7**, DOI: 10.1093/gigascience/gix134 (2017). Gix134, <https://academic.oup.com/gigascience/article-pdf/7/4/gix134/24619986/gix134.pdf>.

234 20. Yu, J. *et al.* A unified mixed-model method for association mapping that accounts for multiple levels of relatedness. *Nat. genetics* **38**, 203–208, DOI: [10.1038/ng1702](https://doi.org/10.1038/ng1702) (2006).

235

236 21. Parisseaux, B. & Bernardo, R. In silico mapping of quantitative trait loci in maize. *Theor. Appl. Genet.* **109**, 508–514, DOI: [10.1007/s00122-004-1666-0](https://doi.org/10.1007/s00122-004-1666-0) (2004).

237

238 22. Chang, C. C. *et al.* Second-generation PLINK: rising to the challenge of larger and richer datasets. *GigaScience* **4**, DOI: [10.1186/s13742-015-0047-8](https://doi.org/10.1186/s13742-015-0047-8) (2015). S13742-015-0047-8, [https://academic.oup.com/gigascience/article-pdf/4/1/s13742-015-0047-8/25512027/13742\\_2015\\_article\\_47.pdf](https://academic.oup.com/gigascience/article-pdf/4/1/s13742-015-0047-8/25512027/13742_2015_article_47.pdf).

239

240

241 23. Zhou, X. & Stephens, M. Genome-wide efficient mixed-model analysis for association studies. *Nat. genetics* **44**, 821–824 (2012).

242

243 24. Zeng, J. *et al.* Signatures of negative selection in the genetic architecture of human complex traits. *Nat. genetics* **50**, 746–753, DOI: [10.1038/s41588-018-0101-4](https://doi.org/10.1038/s41588-018-0101-4) (2018).

244

245 25. Yang, Z., Xu, G., Zhang, Q., Obata, T. & Yang, J. Genome-wide mediation analysis: an empirical study to connect phenotype with genotype via intermediate transcriptomic data in maize. *Genetics* **221**, iyac057 (2022).

246

247 26. Liu, Y. *et al.* Genomic basis of geographical adaptation to soil nitrogen in rice. *Nature* **590**, 600–605, DOI: [10.1038/s41586-020-03091-w](https://doi.org/10.1038/s41586-020-03091-w) (2021).

248

249 27. Falconer, D. S. & Mackay, T. F. C. *Introduction to quantitative genetics* (Harlow: Longman, 1996), fourth edn.

250

251 28. Yang, Z., Xu, G., Zhang, Q., Obata, T. & Yang, J. Genome-wide mediation analysis: bridging the divide between genotype and phenotype via transcriptomic data in maize. *bioRxiv* (2021).

252

253 29. Li, M.-X., Yeung, J. M., Cherny, S. S. & Sham, P. C. Evaluating the effective numbers of independent tests and significant p-value thresholds in commercial genotyping arrays and public imputation reference datasets. *Hum. genetics* **131**, 747–756 (2012).

254

255 30. Ribeiro, P. *et al.* Identification of quantitative trait loci for grain yield and other traits in tropical maize under high and low soil-nitrogen environments. *Crop. Sci.* **58**, 321–331, DOI: <https://doi.org/10.2135/cropsci2017.02.0117> (2018). <https://acsess.onlinelibrary.wiley.com/doi/pdf/10.2135/cropsci2017.02.0117>.

256

257

258 31. Yang, H. *et al.* Temporal and spatial variations of soil c, n contents and c:n stoichiometry in the major grain-producing region of the north china plain. *PLOS ONE* **16**, 1–14, DOI: [10.1371/journal.pone.0253160](https://doi.org/10.1371/journal.pone.0253160) (2021).

259

260 32. Zhu, H., Chen, X. & Zhang, Y. Temporal and spatial variability of nitrogen in rice–wheat rotation in field scale. *Environ. earth sciences* **68**, 585–590, DOI: [10.1007/s12665-012-1762-4](https://doi.org/10.1007/s12665-012-1762-4) (2013).

261

262 **Supplemental Material**

263 **Supporting Tables**

**Table S1. The best linear unbiased prediction (BLUP) values of yield-related traits.**

([https://github.com/jyanglab/Genetics-parameters-for-N-related-traits/blob/main/supp%20tables/Stable1\\_phenotype.xlsx](https://github.com/jyanglab/Genetics-parameters-for-N-related-traits/blob/main/supp%20tables/Stable1_phenotype.xlsx))

**Table S2. GWAS SNPs for cob- and kernel-related traits under different N conditions.**

([https://github.com/jyanglab/Genetics-parameters-for-N-related-traits/blob/main/supp%20tables/Stable2\\_Significant\\_SNPs\\_from\\_GWAS.xlsx](https://github.com/jyanglab/Genetics-parameters-for-N-related-traits/blob/main/supp%20tables/Stable2_Significant_SNPs_from_GWAS.xlsx))

**Table S3. Trait-associated loci for cob- and kernel-related traits under different N conditions.**

([https://github.com/jyanglab/Genetics-parameters-for-N-related-traits/blob/main/supp%20tables/Stable3\\_GWAS\\_Loci.xlsx](https://github.com/jyanglab/Genetics-parameters-for-N-related-traits/blob/main/supp%20tables/Stable3_GWAS_Loci.xlsx))

264 **Supporting Figures**

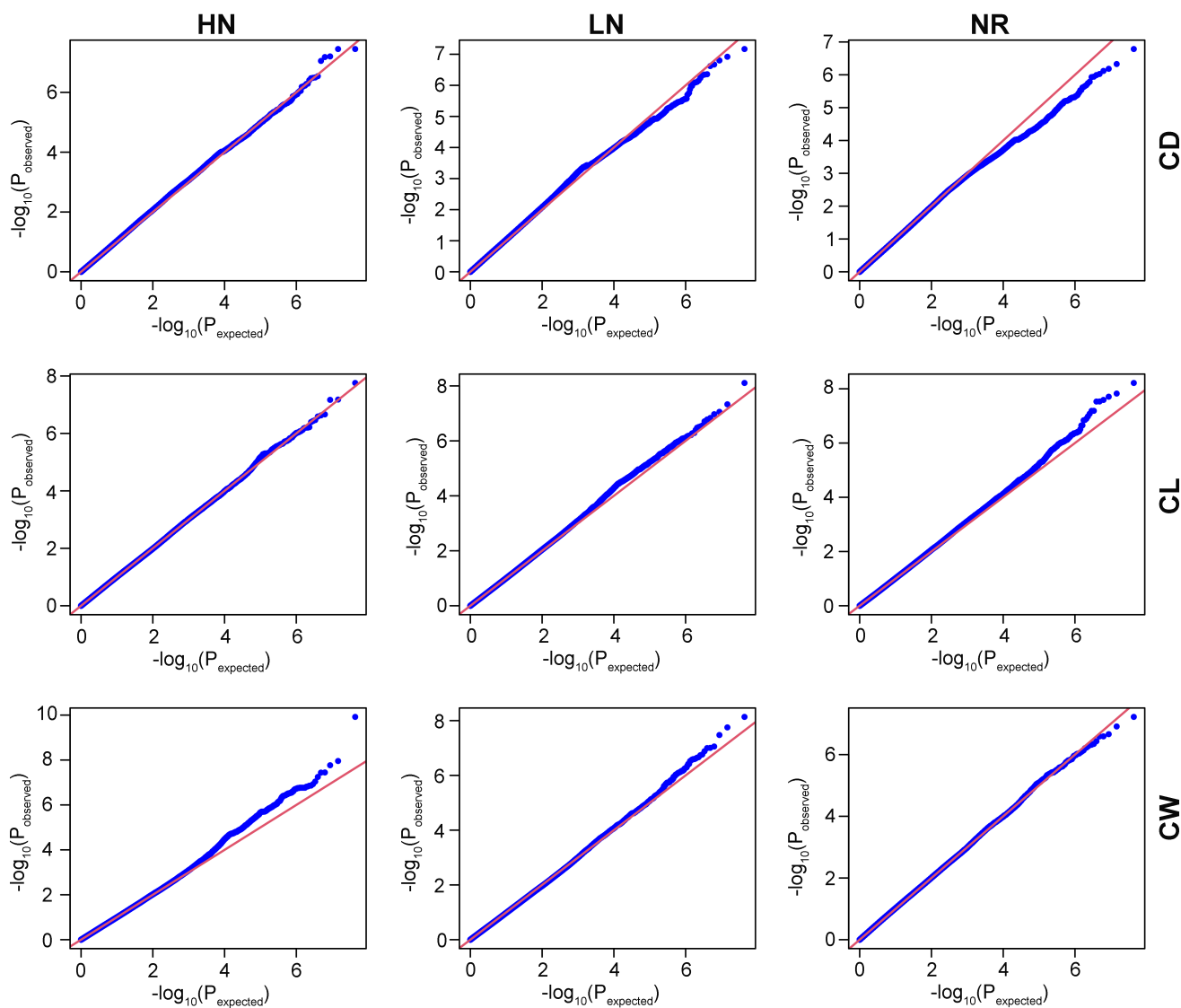


**Figure S1. Quantile-quantile (Q-Q) plots for cob-related traits.** Red diagonal line indicates the expected values and the blue dots represent the observations.

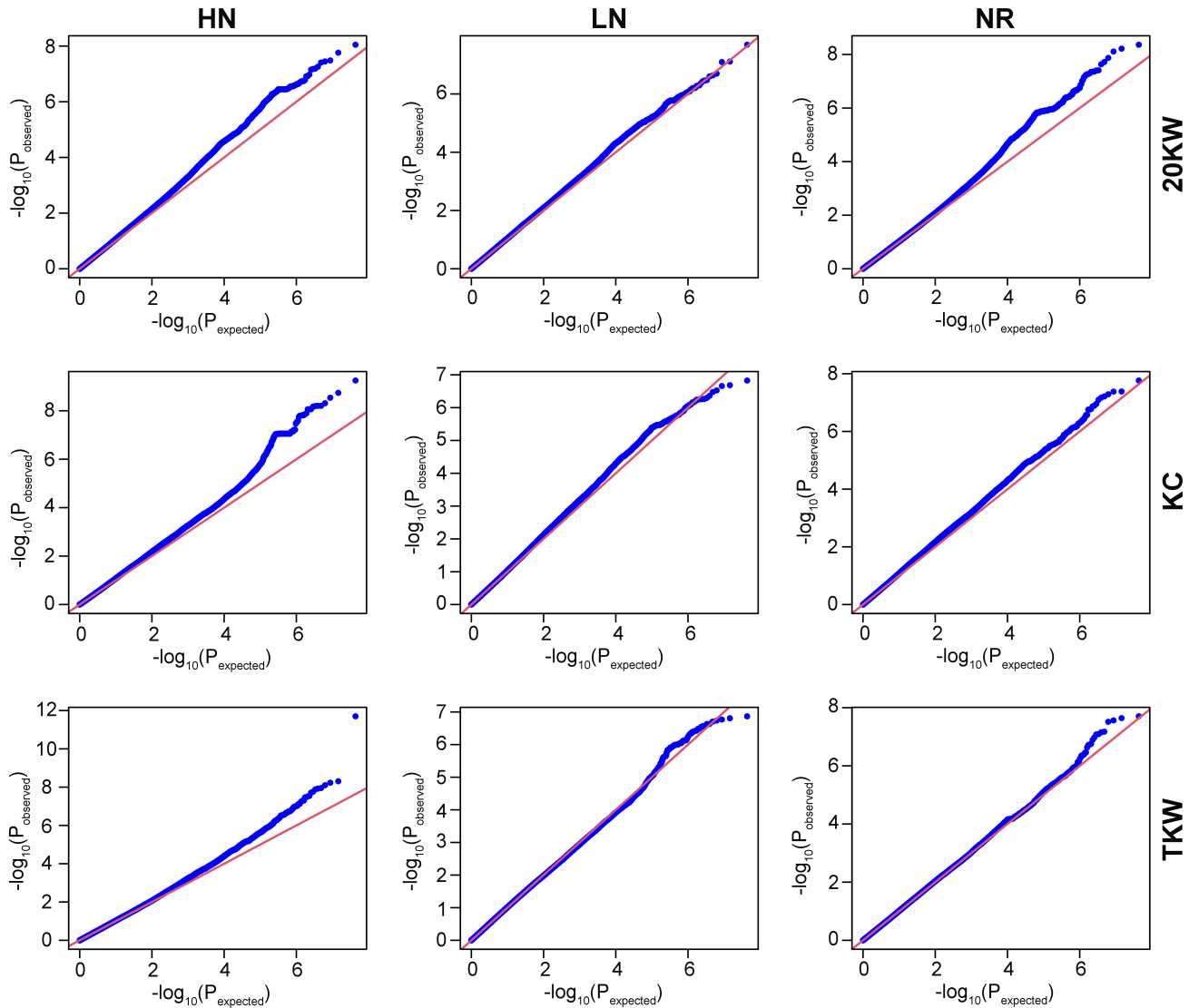


**Figure S2. Quantile-quantile (Q-Q) plots for kernel-related traits.** Red diagonal line indicates the expected values and the blue dots represent the observations.

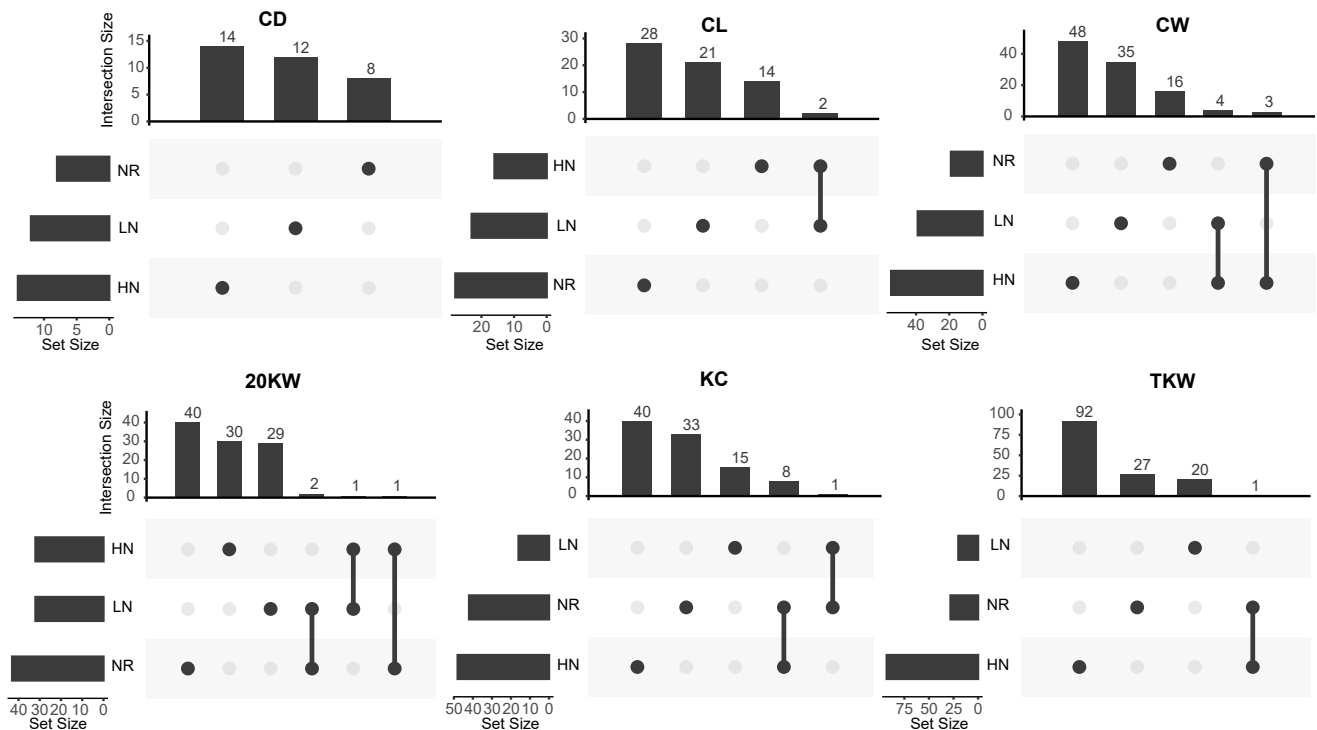


**Figure S3. Overlapping results of trait-associated loci (TALs) for each trait under three different N conditions.**  
Numbers on top of the barplots indicate the number of unique (only dots) and shared (dots and lines) TALs.

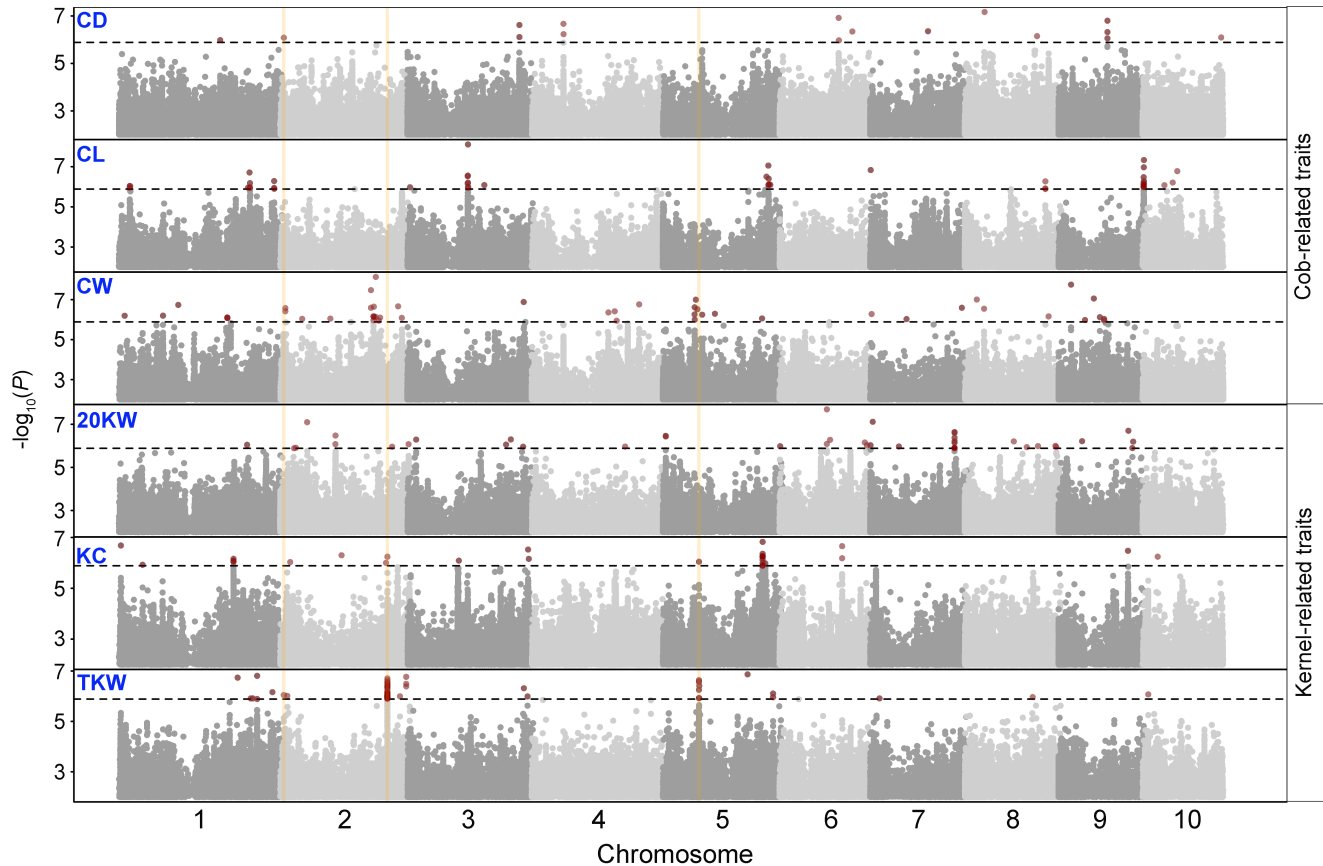


**Figure S4. Stacking Manhattan plot of cob- and kernel-related traits under LN conditions.** The black horizontal dashed line indicates the GWAS threshold. Each red dot above the threshold represents the SNP significantly associated with a trait. The vertical orange lines indicate the overlapped trait-associated loci (TALs).

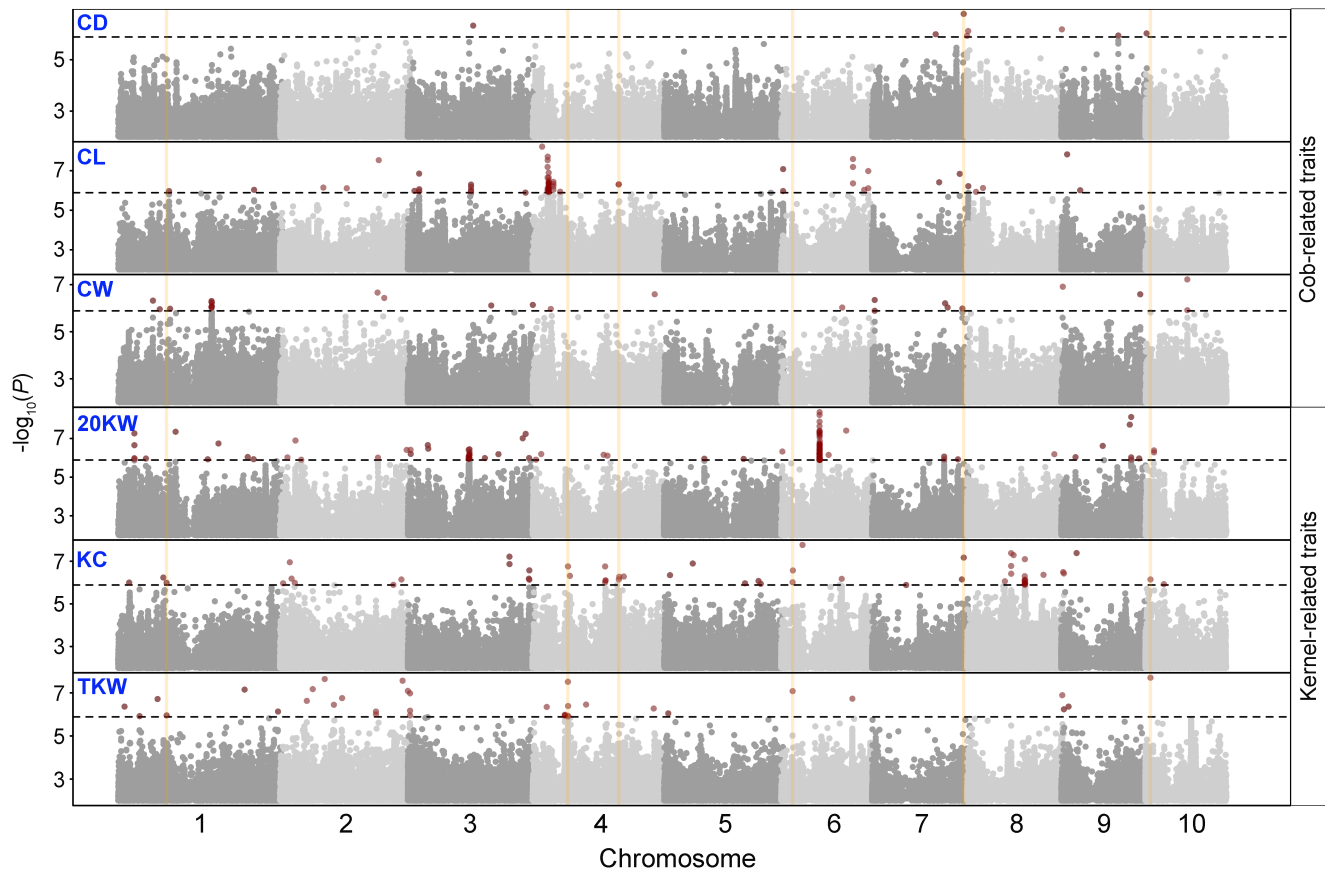


**Figure S5. Stacking Manhattan plot for N-responsive (NR) traits.** The black horizontal dashed line indicates the GWAS threshold. Each red dot above the threshold represents the SNP significantly associated with a trait. The vertical orange lines indicate the overlapped trait-associated loci (TALs).